16

NMR Investigations on Ruggedness of Native State Energy Landscape in Folded Proteins

Poluri Maruthi Krishna Mohan
Department of Chemistry & Chemical Biology,
Rutgers University, New Jersey,
USA

1. Introduction

The ability of proteins to adopt their functional, highly structured states in the intracellular environment during and after its synthesis is one of the most remarkable evolutionary achievements of biology. Deciphering the code of protein self-organization process has been an intellectual challenge for scientists over the past few decades. Although the structure-function paradigm about folded structures and functions remains valid, the role of internal dynamics and conformational fluctuations in protein function is becoming increasingly evident (Bhabha *et al* 2011; Boehr *et al* 2006; Eisenmesser *et al* 2005; Fraser *et al* 2009; Mittermaier and Kay 2006; Parak 2003b; Popovych *et al* 2006; Tzeng and Kalodimos 2009; Whitten *et al* 2005). Further, recent structural and genomic data have clearly shown that not all proteins have unique folded structures under normal physiological conditions. Hence, the way a protein exists, is bound to have a profound effect on its function.

A complete understanding of protein folding process requires characterization of all the species populating along the folding coordinate, these include the unfolded state, the partially folded intermediate states, low energy excited states and the fully folded native state. The most recent and widely accepted model is the 'funnel view' of protein folding (Bryngelson *et al* 1995; Dill and Chan 1997; Onuchic *et al* 1997; Shoemaker *et al* 1999; Wolynes 2005) also known as the 'Energy landscape model' **(Fig. 1)**, which is inclusive of the earlier concepts of 'folding pathways'. According to this model protein folding is a parallel, diffusion-like motion of conformational ensemble on the energy landscape biased towards the native state. This model is free from the Levinthal paradox (Dill and Chan 1997; Levinthal C 1969) as it envisages the process of reaching a global minimum in free energy as a rapid process occurring by multiple routes on a funnel like energy landscape **(Fig. 1)**. This view focuses on the rapid decrease of the conformational heterogeneity in the course of the folding reaction and is based on a statistical description of a protein's potential surface (Wolynes *et al* 1995; Wolynes 2005). The depth in the funnel represents the free energy of the polypeptide chain in fixed conformations and the width indicates the chain entropy **(Fig. 1)**. The funnel becomes narrower in the lower energy region because of the low chain entropy. The broad end of the funnel reflects the heterogeneous unfolded state, while the narrow end represents the supposedly homogeneous native state (Dill and Chan 1997; Dobson and Karplus 1999; Dyson and Wright 2005). Different members of the ensemble

may fold/unfold along independent pathways and their energy profiles could be different. Protein folding theories start from the unfolded state **(Fig. 1)** and encompass a range of topologies like the pre-molten globule, the molten globule and various other ordered or disordered forms as the protein folds down the funnel (Dunker *et al* 2002; Uversky 2002; Uversky 2003).

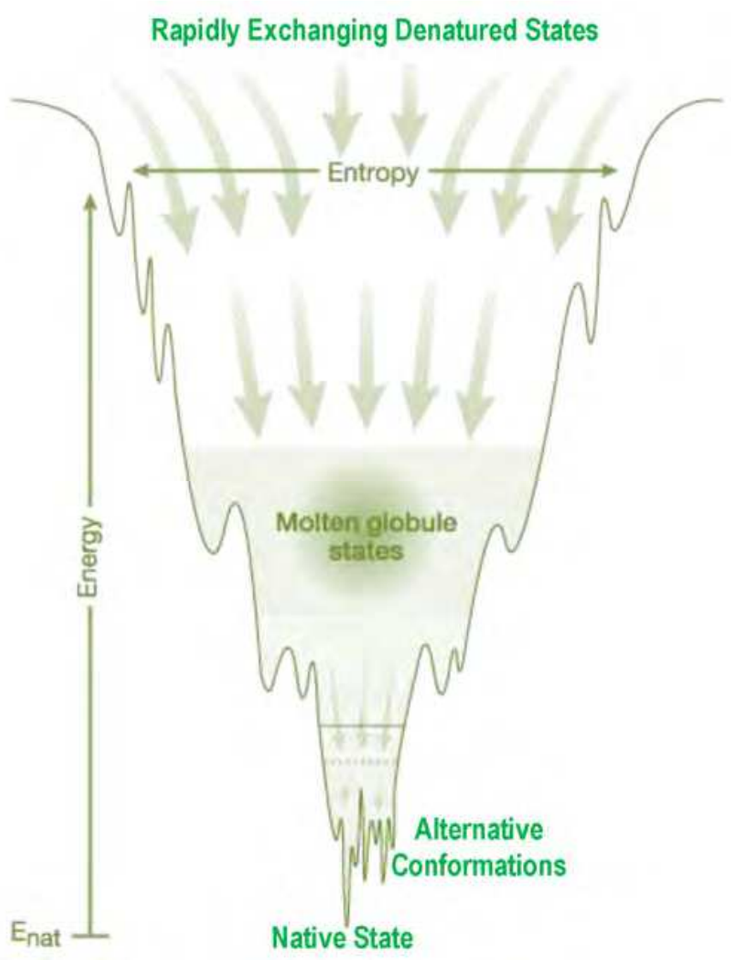

Fig. 1. A schematic energy landscape view of protein folding: The surface of the funnel represents a whole range from the multitude of denatured conformations to the unique native structure (Dill and Chan 1997). The ordered state is the natively folded structure of a protein that has a well defined secondary and tertiary structure. Alternative conformations are higher energy native state conformations and contain all the secondary and tertiary structural characteristics of folded state. Molten globule states are intermediates in the protein folding pathway with compact structures that exhibit a high content of secondary structure, nonspecific tertiary structure, and significant structural flexibility. Random coils are highly unstructured protein denatured states.

In a living cell, a polypeptide chain chooses between three potential fates - functional folding, potentially deadly misfolding and mysterious non-folding (Dobson 2003). This choice is dictated by the peculiarities of amino acid sequence and/or by the pressure of

environmental factors. The biological function of a protein arises as a result of interplay between specific conformational forms, namely, native state (ordered forms), low energy excited states, molten globules, pre-molten globules, and denatured state (random coils). In view of this, it will not be an exaggeration to assume an ensemble existence of all these states at any particular time, their relative abundance being governed by basic thermodynamics. Upon ligand binding or some signaling modification, concentration of one state may increase at the expense of the others. This can explain the fast regulatory steps involved in various biological functions.

Much of structural biology of proteins is so focused on studies of native state, providing detailed atomic descriptions and coordinates of static three-dimensional (3D) structures. A large body of evidence using a diverse spectrum of biophysical methods clearly establishes that proteins are dynamic over a broad range of timescales and such dynamics play critical roles in various biological processes, such as: initial formation of encounter complexes in macromolecular association, target searching in specific protein-protein/protein-DNA recognition, conformational preferences in ligand binding, conformational transitions associated with allostery, the course of enzyme catalysis, intermediates along the protein folding pathway, and early events in self-assembly processes (Bai *et al* 1995; Boehr *et al* 2006; Clore 2011; Dunker *et al* 2002; Eisenmesser *et al* 2005; Feher and Cavanagh 1999; Fraser *et al* 2009; Kitahara *et al* 2005; Korzhnev *et al* 2003; Kumar *et al* 2007; Lambers *et al* 2006; Mohan *et al* 2006; Piana *et al* 2002; Popovych *et al* 2006; Tang *et al* 2008; Villali and Kern 2010). The amplitudes and the timescales of motion that characterize the dynamics of a protein under a given set of conditions can be understood in terms of an 'energy landscape' as described above. Ground-state conformers that occupy the bottom of the energy landscape funnel and are separated from other conformational states by very small kinetic barriers that are easily overcome by thermal energy form the basis of structural studies by NMR (Nuclear Magnetic Resonance Spectroscopy) and X-ray diffraction for last few decades.

In general, the dynamic phenomenon involves the inter-conversion between ground state conformers with higher energy structures known as 'excited states'. The populations of these low-energy excited states/near native states/alternative conformations at equilibrium are very sparse and their lifetimes are short. Moreover, these transient states arising from rare but rapid excursions between the global free energy minimum and higher free energy local minima are extremely challenging to study at atomic resolution under equilibrium conditions since they are effectively invisible to most structural and biophysical techniques including crystallography and conventional NMR spectroscopy (Bhabha *et al* 2011; Boehr *et al* 2006; Eisenmesser *et al* 2005; Fraser *et al* 2009; Mittermaier and Kay 2006; Popovych *et al* 2006; Tzeng and Kalodimos 2009; Whitten *et al* 2005; Clore and Iwahara 2009; Clore 2011). However, a complete understanding of the conformational fluctuations these bio-molecules undergo is essential to gain an insight into their biochemical and biophysical properties. Hence, it is critical to characterize the structural ensembles that describe these functionally important states and the mechanisms by which they interconvert with the ground-state conformers.

Recent developments in NMR, however, have rendered short-lived, sparsely populated states accessible to spectroscopic analysis, yielding considerable insights into their kinetics, thermodynamics, and structures. Over the past decade, new and powerful NMR approaches

such as paramagnetic relaxation enhancement (PRE) (Clore and Iwahara 2009; Clore 2011), relaxation dispersion (RD) (Boehr *et al* 2006; Mittermaier and Kay 2006; Tzeng and Kalodimos 2009) and non-linear temperature dependence of amide proton chemical shifts (Krishna Mohan *et al* 2008; Mohan *et al* 2008b; Tunnicliffe *et al* 2005; Williamson 2003) have emerged and significantly contributed to our understanding of the relationship between structure, dynamics and function of proteins with respect to the excited-state conformers that are sparsely populated and often exist transiently.

In the present chapter the theoretical basis of NMR approach for the curved temperature dependence of amide proton chemical shifts will be discussed in detail. Theoretical simulations will be presented to understand the nature and extent of curvature of the chemical shifts. Further, experimental studies performed till date on different protein systems will be reviewed to demonstrate the curved temperature dependence of amide proton chemical shifts as a tool to detect the low populated near native states/ alternative conformations of the protein residues. Moreover, the significance of these conformational fluctuations will be evaluated with regard to protein function and folding.

2. Theory of curved temperature dependence of amide proton chemical shifts

NMR chemical shift is a sensitive indicator of the environment and molecular conformation. In proteins ^{1}H, ^{13}C and ^{15}N chemical shifts are sensitive to protein secondary structures and are used to deduce the preliminary structural information (Schwarzinger *et al* 2000; Schwarzinger *et al* 2001; Wishart and Sykes 1994; Wishart *et al* 1995; Wüthrich K 1986). The temperature dependence of amide proton chemical shifts in globular proteins has been investigated for over more than three decades by many researchers and continues to be investigated even today (Anderson *et al* 1997; Baxter and Williamson 1997; Cierpicki and Otlewski 2001; Krishna Mohan *et al* 2008). The amide proton chemical shifts are directly proportional to bond magnetic anisotropy (σ^{ani}) and this is crucially dependent on H-bonding, either intramolecular or intermolecular. In the former case, the carbonyl groups, the H-bond acceptors play a crucial role. The bond magnetic anisotropy is proportional to r^{-3} where r is the distance between the affected amide proton and the centre of the bond magnetic anisotropy, which lies close to the oxygen atom in the carbonyl groups (Krishna Mohan *et al* 2008). In case of solvent accessible groups, H-bonding with solvent molecules influences the amide proton chemical shifts. Thus the amide proton chemical shift is critically dependent on the length of the H-bond the proton is engaged in.

When the temperature of the solution is raised, thermal fluctuations increase which results in an increase in the average distance between atoms; X-ray crystallographic studies at several temperatures (98 – 320 K) on ribonuclease-A indicated that the protein volume increases linearly with temperature to an extent of about 0.4% per 100 K (Tilton, Jr. *et al* 1992). Such an increase in the distance between the atoms participating in a H-bond results in weakening of the H-bond. Consequently, chemical shifts of most amide protons move up field when the temperature is increased. Since bond magnetic anisotropy (σ^{ani}) is proportional to r^{-3} and molecular volume (V) is proportional to r^{3}, there is an inverse relationship of their variation with temperature ((σ^{ani}) α 1/V). However, over a small temperature range, (σ^{ani}) may appear to decrease linearly with temperature, and

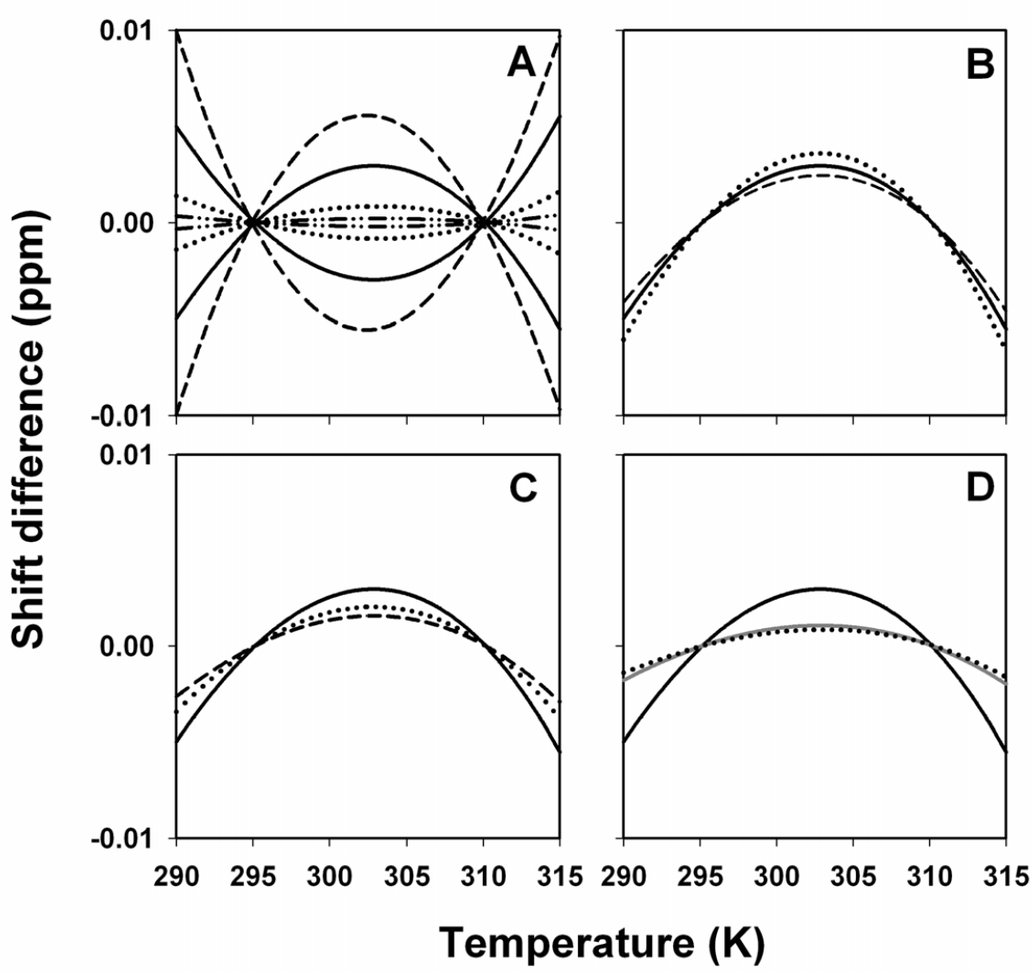

Fig. 2. Simulations of the dependence of H^N chemical shift variation with temperature (290 K – 315 K). In all the calculations shown chemical shifts are calculated and fitted to a straight line. Then the deviations from linearity are used to derive the residual curvatures (Krishna Mohan *et al* 2008; Williamson 2003). **(A)** Different curves show the dependence on free energy difference between the native and the higher energy alternate state: ΔG = 1 kcal/mol (dashed), ΔG = 2 kcal/mol (solid), ΔG = 3 kcal/mol (dotted) and ΔG = 4 kcal/mol (dash double dot dash); for these $T\Delta S$ at 298 K was fixed at 5.1 kcal/mol and ΔH varied as 6.1, 7.1, 8.1, and 9.1 kcal/mol respectively. The chemical shift and gradient parameters are: δ_1 = 8.5 ppm, δ_2 = 8.0 ppm, and g_1 = -2 ppb/K, g_2 = -7 ppb/K for convex shapes and δ_1 = 8.0 ppm, δ_2 = 8.5 ppm, and g_1 = -7 ppb/K, g_2 = - 2 ppb/K for concave shapes. **(B)** The solid curve is the same as in '**A'** (ΔG = 2 kcal/mol); Dashed curve, δ_1 = 8.1 ppm, δ_2 = 8.0 ppm, g_1 = -2 ppb/K, g_2 = -7 ppb/K, ΔG = 2 kcal/mol; dotted curve, δ_1 = 9.0 ppm, δ_2 = 8.0 ppm, g_1 = -2 ppb/K, g_2 = -7 ppb/K, ΔG = 2 kcal/mol **(C)** The solid curve is the same as in '**A'** (ΔG = 2 kcal/mol); dashed curve, δ_1 = 8.5 ppm, δ_2 = 8.0 ppm, g_1 = -2 ppb/K, g_2 = - 4 ppb/K, ΔG = 2 kcal/mol; dotted curve, δ_1 = 8.5 ppm, δ_2 = 8.0 ppm, g_1 = -4 ppb/K, g_2 = - 7 ppb/K, ΔG = 2 kcal/mol. **(D)** The solid black curve (ΔG = 2 kcal/mol) and the dotted curve (ΔG = 3 kcal/mol) are the same as in **'A'**; solid grey curve is for δ_1=8.1 ppm, δ_2=8.0 ppm, g_1 = -2 ppb/K, g_2 = -4 ppb/K with ΔG = 2 kcal/mol.

consequently amide proton chemical shifts would appear to vary linearly with temperature. In BPTI (basic pancreatic trypsin inhibitor) and lysozyme which are known to be extremely stable under a variety of extreme conditions, including temperature, it was indeed observed that the amide proton chemical shifts change linearly with temperature over the ranges, 279-359 K for BPTI and 278 – 328 K for Lysozyme (Baxter and Williamson 1997). Such measurements have been carried out on many other proteins (Cierpicki and Otlewski 2001; Cierpicki *et al* 2002) and the temperature coefficients or the gradients of temperature dependence of the amide protons have been found to span a wide range, -16 to + 4 ppb/K. For a strongly H-bonded amide this value is more positive than -4.5 ppb /K (Baxter and Williamson 1997). This is because the lengthening of the average H-bond distance will be greater for the intermolecular H-bond, such as those with bulk water, than for the intra-molecular H-bonds.

However, if the protein structure is not very rigid, as would be the case for many systems, the chemical shifts would also be influenced by local structural and dynamics changes, and then the temperature dependence of chemical shifts may deviate from linearity. Indeed, in certain situations the amide proton chemical shifts have been seen to be non linearly dependent on temperature, and this has been interpreted to indicate existence of alternative conformations the residues can access (Baxter *et al* 1998; Williamson 2003). Identification of such residues provides a description of the energy landscape of the protein in the native state. The observed curvatures can be theoretically deduced as described in the following paragraphs.

Consider a residue having two conformational states accessible to it i.e., a native state and a higher energy state. Following the discussion in the above paragraphs, each of them can be assumed to have a linear variation of chemical shift with temperature as, $\delta_1 = \delta^0_1 + g_1 T$ and $\delta_2 = \delta^0_2 + g_2 T$, where g_1 and g_2 are the gradients of temperature dependence, δ_1 and δ_2 are the chemical shifts of the native and the excited states respectively, and T is the temperature. If P_1 and P_2 are the corresponding populations of the native and the excited states, the observed chemical shift, δ_{obs}, of the amide proton will be given by,

$$\delta_{obs} = \delta_1 P_1 + \delta_2 P_2 \tag{1}$$

These populations depend on the free energy difference between the two states. If there are more states contributing, then the observed shift will be a weighted average over all the accessible states. It is this complex dependence of chemical shifts on many thermodynamic and other factors, which leads to non linear dependence of chemical shifts on temperature. To understand the influence of these factors, simulations of H^N chemical shift variation are performed with temperature in the range, 290 K – 315 K, using a two state model (Krishna Mohan *et al* 2008; Williamson 2003)

$$\delta_{obs} = \frac{(\delta^0_1 + g_1 T) + [(\delta^0_2 + g_2 T) e^{-(\Delta G/RT)}]}{1 + e^{-(\Delta G/RT)}} \tag{2}$$

where, ΔG is the free-energy difference between the two states, and $\Delta G = \Delta H - T\Delta S$, where, ΔH and ΔS are the enthalpy difference and the entropy difference respectively. The results of the simulations are shown in **Fig. 2**. **Fig. 2A** shows the curves for ΔG ranging from 1 - 4

kcal/mol keeping the gradients and chemical shifts of the native and the excited states constant. Here, it is worthwhile to note that in the chosen temperature range (290 K – 315 K) the curvature almost disappears above ΔG = 3 kcal/mol. **Fig. 2B** and **Fig. 2C** show the dependence of curvature on chemical shift differences and gradient differences respectively, between the native and the excited states, when ΔG is held constant (ΔG = 2 kcal/mol). In **Fig. 2B**, three values of δ_1: 8.5 (reference), 8.1 and 9.0 are considered, keeping the other parameters the same as in **Fig. 2A** for convex shape of curvature. Similarly, in **Fig. 2C**, three combinations of gradients: (g_1,g_2) (ppb/K) = (-2, -7) (reference), (-2, -4) and (-4, -7) are considered keeping the other parameters same as in **Fig. 2A** for convex shape of curvature. From these it is evident that neither the chemical shift difference nor the difference in gradients, by itself changes the curvature to a noticeable extent. A simulation carried out for a combination of changes in 'chemical shift difference' and 'gradient difference' (δ_1=8.1 ppm, δ_2=8.0 ppm, g_1 = -2 ppb/K, g_2 = -4 ppb/K) keeping the free energy constant (ΔG = 2 kcal/mol). This is shown by solid grey line in **Fig 2D**. Interestingly, this curve almost exactly overlaps with the curve for which ΔG = 3 kcal/mol in **Fig. 2A** which has a lower curvature compared to that of the curve with ΔG = 2 kcal/mol; for ease of comparison, the corresponding curve from **Fig. 2A** is redrawn in **Fig. 2D** as a dotted line. This clearly suggests that although the appearance of curvature confirms the presence of alternative states, the lack of curvature does not necessarily imply the absence of low energy excited states. These theoretical simulations will be of great help for interpreting the experimental results on temperature dependence of amide proton chemical shifts.

3. Investigations on native state ruggedness of complex protein systems

A deep well, the bottom of which corresponds to the native state would imply high stability of the native state **(Fig. 1)**. In contrast, a potential well with low lying excited states for the native state would be shallow, and this would have significant influence on the dynamics, structural adaptability, or susceptibility of the protein to various functions (Agarwal 2005; Boehr *et al* 2010; Eisenmesser *et al* 2005; Feher and Cavanagh 1999; Kitahara *et al* 2005; Korzhnev *et al* 2003; Parak 2003a; Piana *et al* 2002; Tobi and Bahar 2005). Application of small environmental perturbations such as small concentrations of chemical denaturants, change in pressure, pH change etc., is often useful to investigate the preferential sensitivities of different residues to external perturbations, while the protein itself remains entirely in the native state ensemble (Akasaka 2006; Baxter *et al* 1998; Chatterjee *et al* 2007; Kumar *et al* 2007; Mohan *et al* 2006; Piana *et al* 2002). In fact, these environment sensitive residues of polypeptide chains adopt unique 3D structures, they access various near native states which are structurally similar and energetically closer to the native state. These low populated alternative conformations dictate the ruggedness of the native structure and its biological function.

3.1 Differential native state conformational fluctuations in calcium sensor proteins

Calcium ion plays a crucial role in the regulation of various biological processes. To perform several of its functional activities, Ca^{2+} binds to different protein molecules, which are called as calcium binding proteins (CaBPs) (Heizmann and Schafer 1990). CaBPs with EF-hand motif (EF-CaBPs) belong to a growing sub family of CaBPs (Ababou and Desjarlais 2001; Bhattacharya *et al* 2004; Heizmann 1992; Nelson and Chazin 1998). The EF-hand motif

represents the canonical Ca^{2+} binding motif that consists of a contiguous 12 amino-acid residue long loop flanked by two helices (Kretsinger and Nockolds 1973; Strynadka and James 1989). The EF-CaBPs are broadly classified as Ca^{2+} sensors and Ca^{2+} buffers. Ca^{2+} sensors (Finn *et al* 1995; Hanley and Henley 2005; Hilge *et al* 2006; Shaw *et al* 1990; Vinogradova *et al* 2005) such as Calmodulin (CaM), Troponin C (TnC) etc., undergo huge conformational change upon binding to Ca^{2+} whereas, the Ca^{2+} buffers (Hackney *et al* 2005; Lambers *et al* 2006; Rosenbaum *et al* 2006; Vinogradova *et al* 2005) such as Calbindin D_{9k},

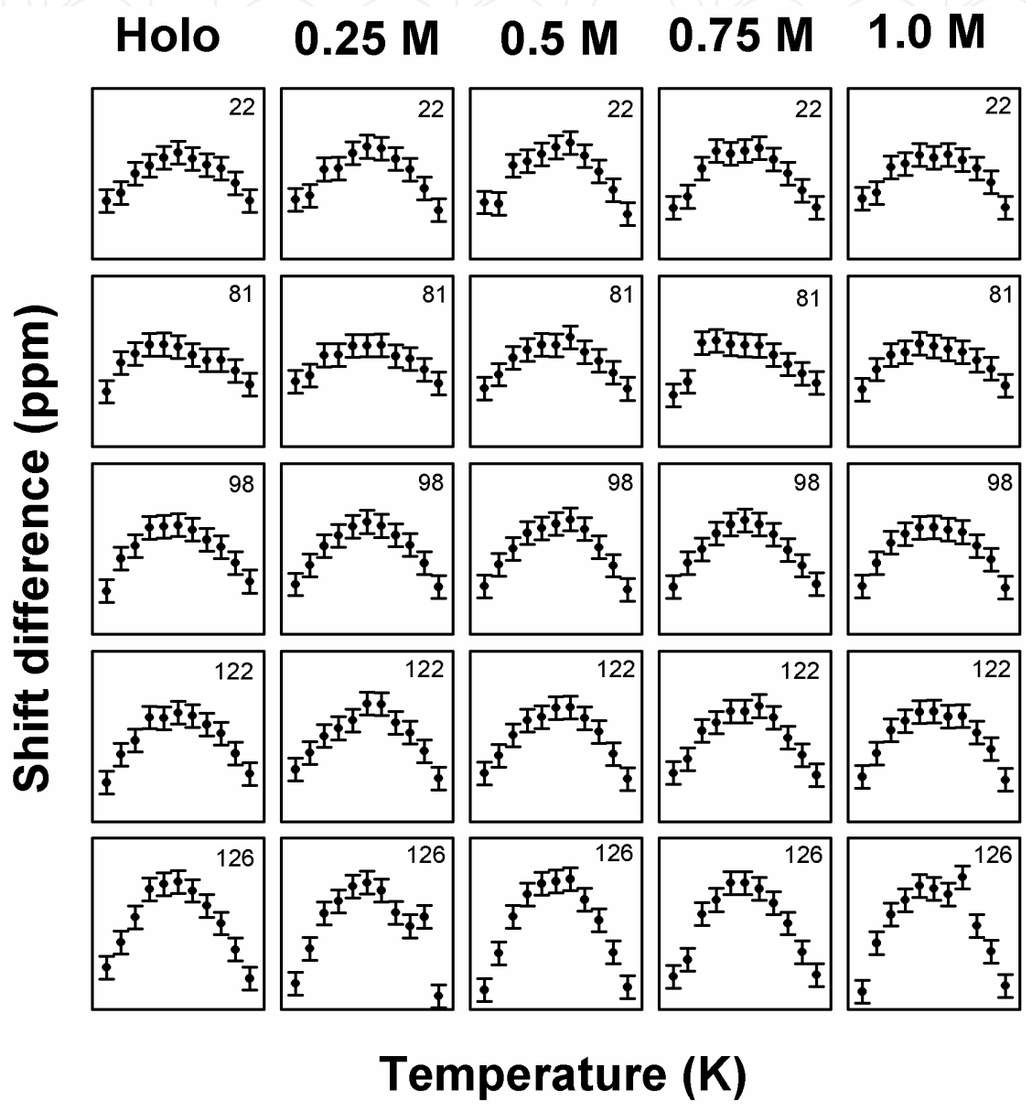

Fig. 3. Illustrative examples for the residues showing nonlinear temperature dependence of backbone $^{1}H^{N}$ chemical shifts in *Eh*CaBP as measured in native state and at different concentrations of GdmCl. The measured chemical shifts were fitted to a linear equation. The residuals (observed value – calculated value according to the linear fit) have been plotted against temperature; total scale of y-axis is 0.06 ppm: +0.03 to -0.03 centered at zero, and the temperature range is 280 K – 335 K. The error bars give an indication of the approximate error in measured chemical shifts (±0.004 ppm).

undergo modest conformational changes upon Ca^{2+} binding. In the current section the experimental evidence for the native state ruggedness on a Ca^{2+} sensor protein from the protozoan *Entamoeba histolytica* (*Eh*CaBP), an etiologic agent of amoebiasis has been demonstrated (Atreya *et al* 2001; Bhattacharya *et al* 2006).

As an illustration, **Fig 3** shows the experimentally measured temperature dependence of backbone proton ($^1H^N$) chemical shifts for few residues in the protein carried out in the temperature range 280 K – 335 K by recording temperature dependent HSQC spectra (Mohan *et al* 2008b). As evident from **Fig. 3**, the observed curvatures are different for different residues. These convex and the concave shapes (Mohan *et al* 2008b; Krishna Mohan *et al* 2008; Williamson 2003) reflect on different kinds of structural perturbations in the excited state compared to the native state as described above in theoretical simulations and illustrated in **Fig 2**. A summary of all the non-linear temperature dependences observed in *Eh*CaBP at different concentrations of GdmCl is given in **Fig. 4**.

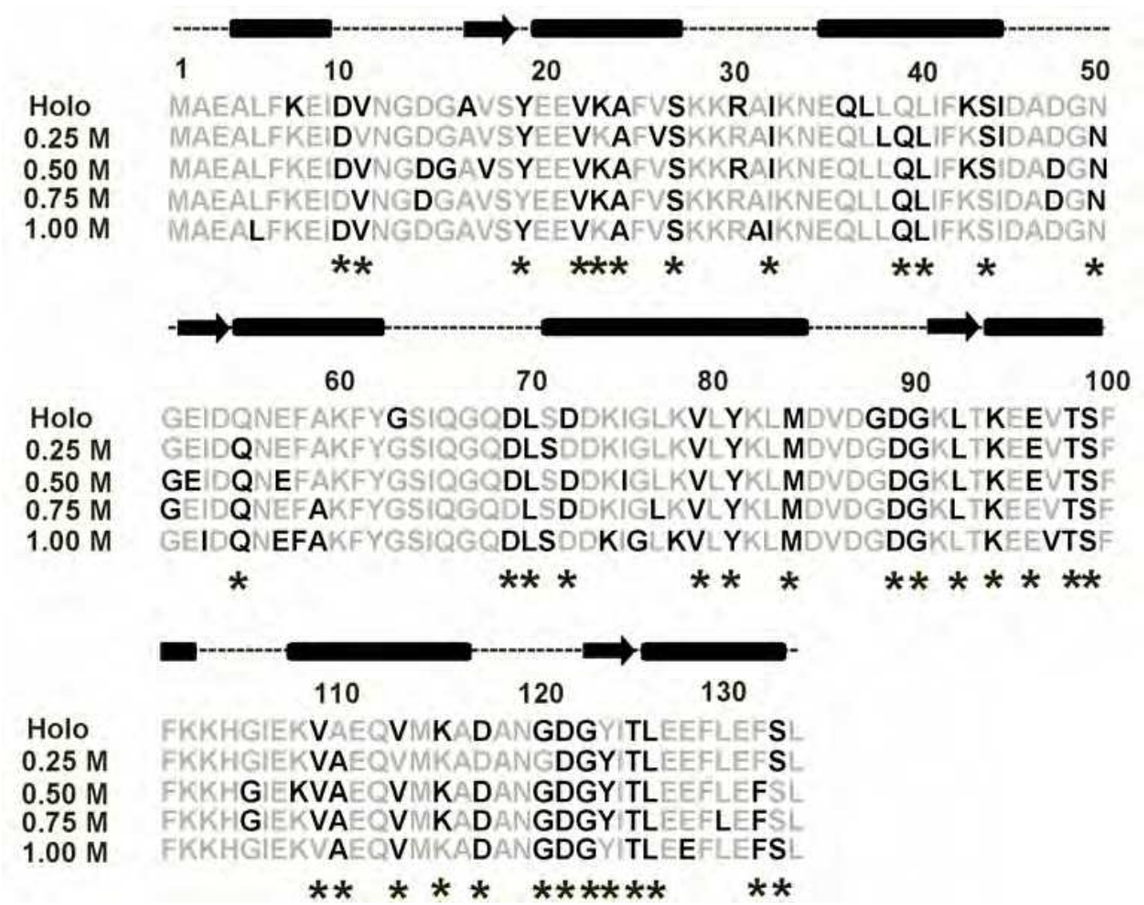

Fig. 4. Residues showing nonlinear temperature dependence of amide proton chemical shifts (black) in the native protein and at different concentrations of GdmCl were shown on the primary sequence of the polypeptide chain. The native secondary structures are shown by arrows (β strands) and cylinders (α helix). Residues accessing alternative conformations at least 3 out of 5 measured GdmCl concentrations are marked with asterisks along the polypeptide chain.

The number of residues accessing alternative states at different concentrations of GdmCl in *Eh*CaBP is (0 M (holo) – 41; 0.25 M – 35; 0.5 M – 50; 0.75 M – 39 and 1.0 M – 42) **(Fig 4)**. The total number of residues which access alternative conformations at least 3 out of 5 measured GdmCl concentrations turned out to be 39 (residues shown with asterisks in Fig. 3), implying that ~ 30 % (39 out of 134) of the residues are accessing alternative conformations. The theoretical simulations described above suggest that the observed curvatures are ~ 2-3 kcal/mol. All these residues are shown in **Fig. 5** on the 3D structure of the protein. Further, the extent of curvatures of individual residues increases or decreases with change in concentration of GdmCl **(Fig.3)** (Williamson 2003). The residues that become more curved with the increasing concentrations of GdmCl are most likely due to the presence of alternate states which are more similar in energy, or more different in shift or gradient to the corresponding native state. This is primarily an off-shoot of contracted unfolding energy landscape in the presence of GdmCl since the GdmCl is not expected to change the nature of the alternative state. Whereas the decrease of curvature can be explained by considering more than one alternative states within 5 kcal/mol, or have an alternative state that becomes very close to native state as GdmCl is increased.

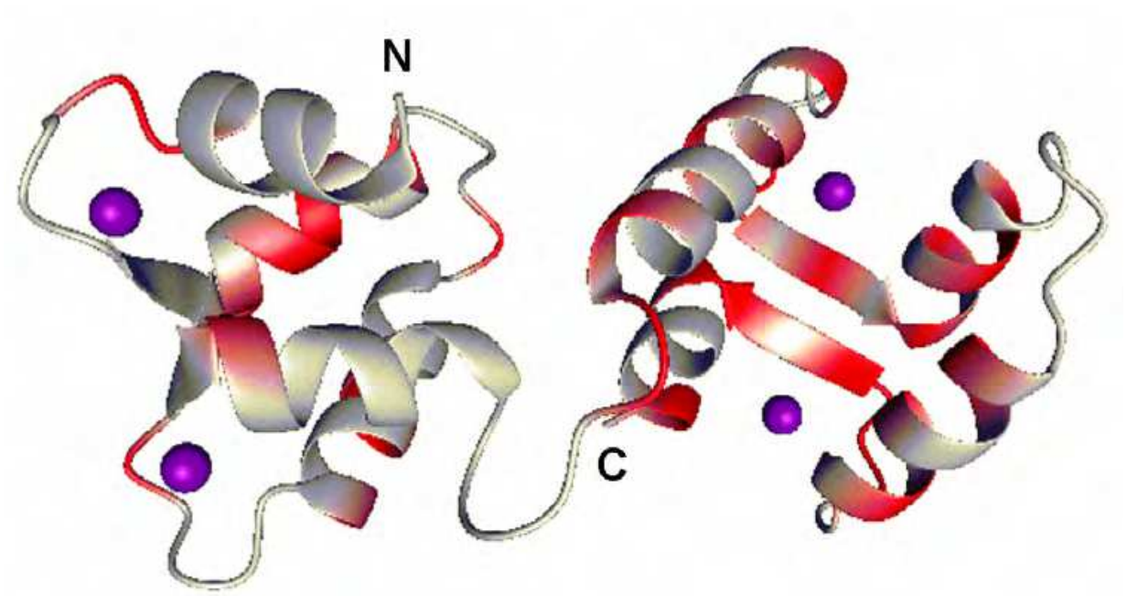

Fig. 5. Residues exhibiting curved temperature dependence at least three out of five concentrations of GdmCl measured in *Eh*CaBP are marked with red color on the 3D structure of the protein (PDB Id: 1JFK).

It is interesting to note that the low energy excited states detected in *Eh*CaBP are not uniformly distributed along the polypeptide chain; different segments of the protein have their own intrinsic preferences to access the alternative conformations. Out of the 39 residues which access low energy excited states, 7 residues belong to EF-hand I; 5 to EF-hand II; 11 to EF-hand III; 13 to EF-hand IV and 3 to the interconnecting loops **(Fig.4)**. It is evident from the data that the density of the conformational fluctuations in the C-terminal domain (24 residues) are twofold compared to the N-terminal counterpart (12 residues)

(**Fig. 4**). This suggests that the C-terminal domain is more flexible and susceptible to structural rearrangements. Further some novel features have been observed in the locations of alternative conformations. The residue at the 5th position of the calcium binding loop (Asp/Asn) that coordinates with Ca^{2+} shows alternative conformations consistently in all the EF-hands. The Gly-6 (the residue at 6th position in the calcium binding loop), which acts as a hinge in the calcium binding loop accesses alternative states in both EF III (Gly-90) and EF IV (Gly-122) hands. Among the calcium binding loops, the IV EF-loop is found to be the most dynamic with maximum number of residues (6 residues out of 12 residue loop) access low energy excited states. This loop has relatively low affinity towards Ca^{2+} compared to the other three loops as demonstrated earlier by the EGTA titration (Mukherjee *et al* 2005), though highly specific for Ca^{2+}. Moreover, recently it has been observed that IV EF-loop also differs with the remaining three EF-loops in the case of Mg^{2+} binding as evidenced by the Mn^{2+} titration (Mukherjee *et al* 2007a). Thus from all the discussion, it can be established that the native state of *Eh*CaBP is rugged due to accessing of various alternative states and the ruggedness is more in the C-terminal domain compared to that in the N-terminal domain. It is interesting to note that among the four EF hands, EF-hands I and II belonging to the N-terminal domain show different conformational dynamics from that of EF-hands III and IV belonging to the C-terminal domain (Mohan *et al* 2008b; Mukherjee *et al* 2007b).

Recently Chandra et al (Chandra *et al* 2011) measuring nonlinear temperature dependence of the backbone amide proton chemical shifts on non-myristoylated (non-myr) and myristoylated (myr) neuronal calcium sensor-1 (NCS-1). The authors reported that ~20% of the residues in the protein access alternative conformations in non-myr case, which increases to ~28% for myr NCS-1. These residues are spread over the entire polypeptide stretch and include the edges of α-helices and β-strands, flexible loop regions, and the Ca^{2+}-binding loops. Besides, residues responsible for the absence of Ca–myristoyl switch are also found accessing alternative states. The C-terminal domain is more populated with these residues compared to its N-terminal counterpart. Individual EF-hands in NCS-1 differ significantly in number of alternate states. Such differences in the conformational dynamics between the two domains and among the EF-loops have significant influence on the specificity and affinity of the metal binding properties and also have implications to domain dependent calcium signaling pathways of calcium sensor proteins (Mohan *et al* 2008b; Mukherjee *et al* 2007b).

3.2 Near native states and structure adaptability of dynein light chain protein

Dynein light chain protein (DLC8), a 10.3 kDa protein (89 residues) is the smallest subunit of the Dynein motor complex. DLC8 is a dimer at physiological pH and a stable monomer below pH 4.0 (Barbar and Hare 2004; Mohan *et al* 2006; Nyarko *et al* 2005). The differences between the monomeric and dimeric structures are, (i) the β3 strand in the dimer loses its secondary structure on dissociation to the monomer, and (ii) the helices α1 and α2 and the strands β1 and β2 get shortened by two residues (Liang *et al* 1999; Makokha *et al* 2004). DLC8 dimer acts as a cargo adapter and recognized as interactive "protein hub" (Barbar 2008). The dimer binds the target molecules in an anti-parallel β-strand fashion through its β3-strand, whereas the monomer form of DLC8 is not capable of binding to target proteins

(Alonso *et al* 2001; Fan *et al* 2001; Fan *et al* 1998; Fuhrmann *et al* 2002; Jaffrey and Snyder 1996; Lo *et al* 2001; Naisbitt *et al* 2000; Puthalakath *et al* 1999). This property is expected to have a regulatory role in the protein function.

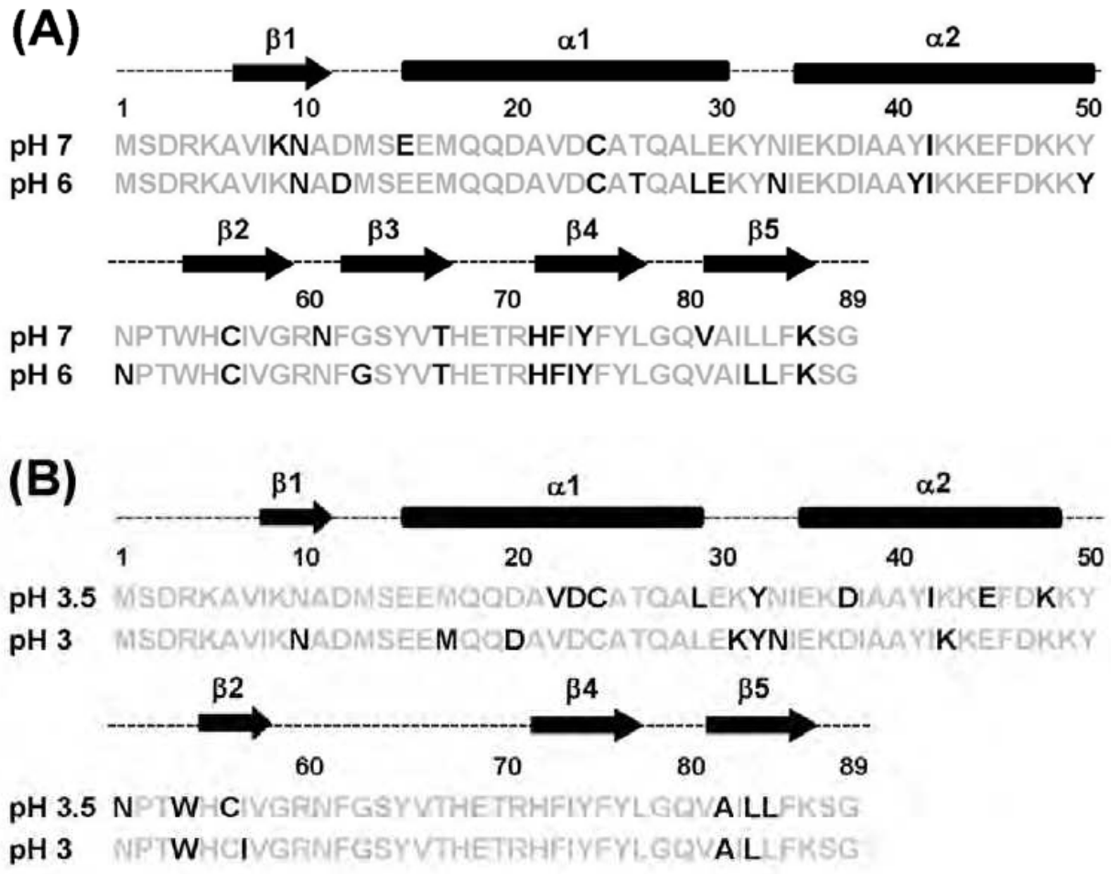

Fig. 6. Residues showing non linear temperature dependence of amide proton chemical shifts (black) in the temperature range is 290 K – 315 K along the polypeptide chain. The results are shown for pH 7.0 and 6.0 **(A)** and for pH 3.5 and 3.0 **(B)**. The arrows (β strands) and cylinders (α helix) indicate native secondary structures.

Temperature dependence of the amide proton chemical shifts in the DLC8 dimer (pH 7) and in the monomer (pH 3) has been measured in the temperature range 290-315 K (Krishna Mohan *et al* 2008). Among the above mentioned environment perturbations, pH variation is a mild perturbation and in general it changes the protonation states of the various residues depending on the chosen pH range. In order to identify the pH sensitive conformational dynamics in DLC8 protein the temperature dependence of the amide proton chemical shifts in both the dimer and the monomer were measured at slightly different pH conditions i.e., dimer at pH 6 and monomer at pH 3.5. A summary of all these results at various pH values i.e., pH 7 and 6 for the dimer and pH 3.5 and 3 for the monomer are shown in **Fig. 6**. Comparison of **Figs. 6A** and **6B** reveals that the residues accessing alternative conformations

have many differences between the dimer and the monomer. The number of residues accessing alternative conformations in the dimer at pH 7 and 6 are 13 and 21 respectively **(Fig.6A)**. **Figs. 7A** and **7B** display the locations of these residues on the native structures of the protein. Likewise, the number of residues accessing alternative conformations in the monomer at pH 3.5 is 15 and that at pH 3 is 11 **(Fig.6B)**. The locations of these residues are marked with red color on the native structure of the monomeric protein in **Figs. 7C** and **7D** respectively.

The differences observed in the positions of the residues accessing alternative conformations in the dimer and in the monomer due to small pH perturbations provide insights into the sensitivity of the conformational fluctuations due to environment perturbations in the two cases. In fact, the perturbation of the dimer landscape would have functional significance since small pH differences are known to exist in different parts of a cell (Spitzer and Poolman 2005; Stewart *et al* 1999; Swietach and Vaughan-Jones 2004; Swietach *et al* 2005; Vaughan-Jones *et al* 2002; Willoughby and Schwiening 2002; Zaniboni *et al* 2003). It is evident from **Figs. 7A** and **7B** that several of the residues that access low energy excited states are surrounding the dimer interface of the molecule which is also the cargo binding site (Krishna Mohan *et al* 2008; Liang *et al* 1999). It can be envisaged that the observed sensitivity of conformational dynamics at the dimer interface due to small environmental perturbations can significantly influence the cargo binding nature of the protein. Likewise, in the monomer **(Figs. 7C** and **7D)** (Krishna Mohan *et al* 2008; Liang *et al* 1999), noticeable differences have been observed in both α1 and α2 helices. Interestingly, the α2 helix participates in several inter-monomer contacts once the dimer is formed and hence its sensitivity to small perturbations may have a crucial role for the proper formation/folding of the functional dimer.

3.2.1 Relationship between sequence, structure and pH sensitivity of DLC8 landscapes

The roughness of the energy landscape and the consequent fluctuations in the native state of a protein is a reflection on the nature of the interactions between the side chains of the different amino acid residues in the three dimensional structure of the protein. While this is not generally predictable, some insights may be obtained in some cases by closely examining the structure and the properties of the amino acids along the sequence. For example, the behaviors of residues with titratable groups, which are likely to be affected by a pH perturbation, can provide useful clues. An observed perturbation at such locations would indicate that conformational fluctuations could be arising due to existence of species with different protonation states; a change in the protonation state of a side–chain causes a local change in the electrostatic potential, and thereby results in some population of an alternative conformation on energetic considerations. Inter-conversion between the major population and the minor population so created leads to the so-called conformational fluctuations.

In the above background it is interesting to note that most of the residues with titratable groups in the side chains in DLC8 **(Fig.7E)** are located in the regions which are exhibiting conformational fluctuations, and hence, their perturbation by small pH changes provides useful mechanistic insights. In the case of the dimer, the sensitivity of conformational

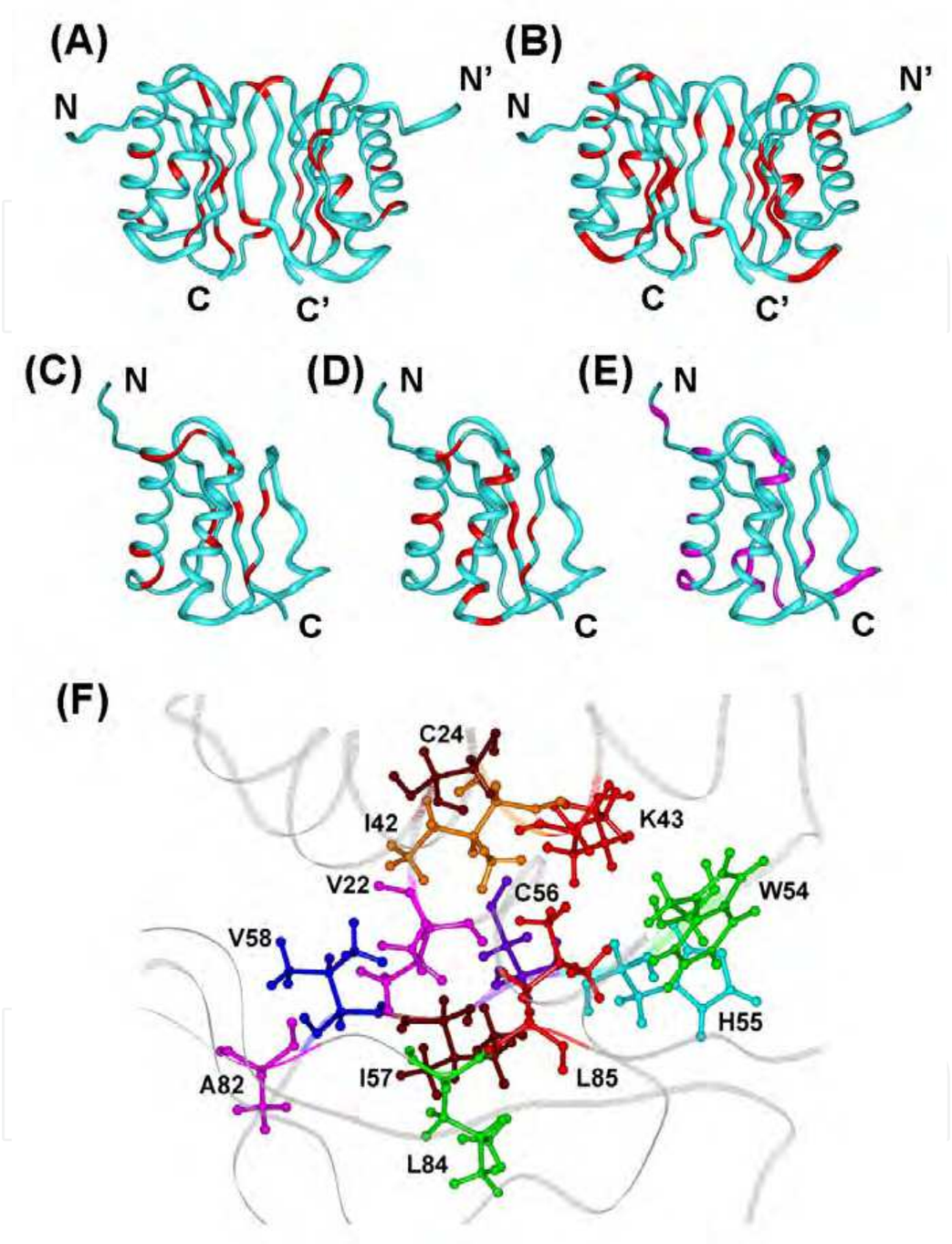

Fig. 7. Residues exhibiting curved temperature dependence in DLC8 dimer **(A)** pH 7.0, (**B)** pH 6.0 (PDB Id: 1f3c) and in monomer **(C)** pH 3.0, (**D)** pH 3.5 (PDB Id: 1hrw), are coloured red on the three dimensional structure of the protein. **(E)** Positions of all the titratable groups in the pH range 7.0 to 3.0 (Aspartates, Glutamates and Histidines) are marked with pink color on the monomer structure (PDB Id: 1rw). **(F)** Zooming in on a particular region surrounding β2 strand in the NMR structure of the monomer (PDB Id: 1rhw) to show the side chain interactions. Only a few residues in α1, α2 and β5 are shown for the sake of clarity.

dynamics can be readily traced to partial protonation of the His side chains as described earlier (Mohan *et al* 2006; Nyarko *et al* 2005). There will be inter-conversions between charged and neutral His and there will also be charge-charge repulsions. These will cause fluctuations in local electrostatic potentials and consequently in local side chain packing, which in turn will affect the main chain conformations. Among the three histidines, His 55 (pK 4.5,), His 68 and His 72 (both have pK of 6.0, (Mohan *et al* 2006; Nyarko *et al* 2005), the latter two would be the major contributors to the observed differences in the fluctuations of the native state in the pH range of 6-7.

In the case of DLC8 monomer His 68 and His 72 do not have any effect on the observed differences as they are completely protonated below pH 4.0. On the other hand His 55 (pK 4.5, (Mohan *et al* 2006; Nyarko *et al* 2005)), would have a significant effect. At pH 3.5 the side chain of His 55 will be protonated to the extent of 90 % and exchange between protonated and free His will contribute to a local dynamics. The environmental perturbation due to this dynamics would get relayed through the β2 strand and the α1, α2 helices and the β5 strand due to the close packing of the side chains in the protein structure **(Fig. 7F)**. The side chains for a few residues of α1, α2 and β5 are shown in the figure and all of these residues are seen to exhibit curved temperature dependence. At pH 3.0, the population of protonated His will increase and this results in the observed perturbation differences. Similarly, the perturbations at the other titratable groups such as aspartates and glutamates in the α1 and α2 helices **(see Fig. 7E)** would also cause local relays and contribute to the accessibility of different low energy excited states. All these influence the native energy landscape of the protein.

3.3 Conformational fluctuations at the phosphorylation site of dynein light chain protein

Recent studies on p21-activated kinase 1 (Pak1), revealed DLC8 as its physiological interacting substrate (binding sites aa 61-89) and the phosphorylation site at Ser 88 (Vadlamudi *et al* 2004). Pak1 phosphorylation of DLC8 on Ser 88 controls vesicle formation and trafficking functions, whereas mutation of Ser 88 to Ala (S88A) prevents macropinocytosis (Song *et al* 2008; Song *et al* 2007; Vadlamudi *et al* 2004; Yang *et al* 2005). Further, DLC8 phosphorylation by Pak1 prevents the interaction with apoptotic protein Bim and plays an essential role in cell survival (Vadlamudi *et al* 2004) and also promotes the dissociation from Intermediate chain (IC74) and hence regulates the assembly of the motor complex (Song *et al* 2007). All these results highlight any perturbation at or near the interface is likely to affect the biological function. Intuitively, the remote effects of any perturbation in a protein must be a consequence of a strong network of interactions which may cause rapid relay of perturbations from any one particular site on the protein structure. However, specific knowledge of how the perturbations travel will be essential in each case to understand the specificities of interactions. In general, perturbations are often introduced deliberately in the form of specific mutations in an attempt to understand the regulatory roles of specific residues involved in target recognition, structural architecture, stability, aggregation and folding features of the wild type protein (Buck *et al* 2007; Frankel *et al* 2007; Grant *et al* 2007; Ishibashi *et al* 2007; Piana *et al* 2008; Riley *et al* 2007; Stollar *et al* 2003).

The phosphorylation site Ser 88 represents an unusual behavior. To understand the conformational behavior phosphorylation site, the amide proton temperature coefficients of

Ser 88 in the WT dimer with those of Ala 88 in the S88A mutant and of Ser 88 in the DLC8 monomer (at pH 3) are measured (Mohan and Hosur 2008). The plots of temperature dependence for these residues are shown in **Fig. 8A**. The measured temperature coefficients are -19.8 ± 0.3, -9.3 ± 0.2 and -5.6 ± 0.1 ppb/^{o}C for Ser 88 in WT dimer, Ala 88 in S88A mutant and Ser 88 in DLC8 monomer respectively. In general the temperature coefficients range between (-2 to -4) ppb/K for a strongly H-bonded amide protons and between (-5 to -10) ppb/K for an exposed solvent accessible (random coil) amide protons (Baxter and Williamson 1997). The values obtained in the case of S88A mutant and DLC8 monomer clearly indicate that the aa 88 is solvent exposed and not strongly hydrogen bonded. On the other hand, a large value of -19.8 ± 0.3 ppb/^{o}C suggests that the environment of Ser 88 in WT dimer is highly susceptible to perturbation. None of the other residues, either in WT monomer or in S88A mutant, showed such a huge temperature coefficient value (Baxter and Williamson 1997; Mohan and Hosur 2008). Williamson et al reported such a large value of temperature coefficient in the herpes simplex virus glycoprotein D-1 antigenic domain (Williamson *et al* 1986) and the experiments demonstrated by Andersen et al (Andersen *et al* 1992) suggested that this amide proton was in fact involved in a transient hydrogen-bonded structure, and thus the large temperature coefficient could be attributed to a loss of secondary/tertiary structure on heating. If the large temperature coefficient of Ser 88 is a consequence of transient hydrogen-bonding and due to loss of secondary/tertiary structure, then Ser 88 should exhibit conformational fluctuations (alternative states). The presence of alternative states for Ser 88 has been tested on Ala 88 residue of S88A mutant and Ser 88 in DLC8 monomer and dimer **(Fig. 8B)**. It is evident that Ser 88 in WT dimer does show a curved temperature dependence of amide proton chemical shifts. Thus, it can be concluded that the amide proton in Ser 88 in WT DLC8 dimer is transiently H-bonded; that it is not a stable H-bond was independently inferred from deuterium exchange studies (Mohan and Hosur 2008; Mohan *et al* 2008a). Moreover, the dimeric structure suggests that the amide group of Gly 89 is very close (~ 2.6 Å) to the backbone nitrogen of Ser 88 suggesting a possibility of potential transient H-bonding.

The mechanism for the relay of perturbations from the Ser 88 site can be envisaged by understanding the close side chain packing. The side chain packing of perturbed residues and Ser 88 are shown in **Fig. 8C**. The crystal structure shows that Ser 88 OG atom is packed against the imidazole ring of His 55 and in addition forms a hydrogen bond with the backbone carbonyl of Ser 88' (Ser 88 of other monomer) (Liang *et al* 1999). From **Fig. 8C** it is evident that Ser 88 is buried inside and packed over side chains of crucial residues at the dimer interface. A closer look at Ser 88 environment in **Fig. 8C** depicts that Ser 88 is closely packed against the side chains of Thr 67, His 68 and Glu 69 of both the monomers in the dimer. Furthermore, the distance measurements between the back bone and side chain atoms of Ser 88 and those of Thr 67, His 68, Glu 69 and Thr 70 indicated that several atoms of Glu 69 are very close (~ 2 – 4 Å), whereas, for residues Thr 67, His 68, Thr 70 there is at least one atom in the distance range of 4 -6 Å. All of these residues are perturbed by the S88A mutation as seen from the chemical shift data. The other perturbed residues are slightly farther (> 6 Å). All these are shown in a color coded manner in **Fig. 8C**. This qualitative analysis provides a mechanistic insight into the relay of perturbation from the phopshorylation site; Glu 69 is most easily perturbed and the disturbance then runs on both sides at the dimer interface. Then, from Tyr 65 the relay spreads to Lys 44 which is engaged in a side chain H-bond.

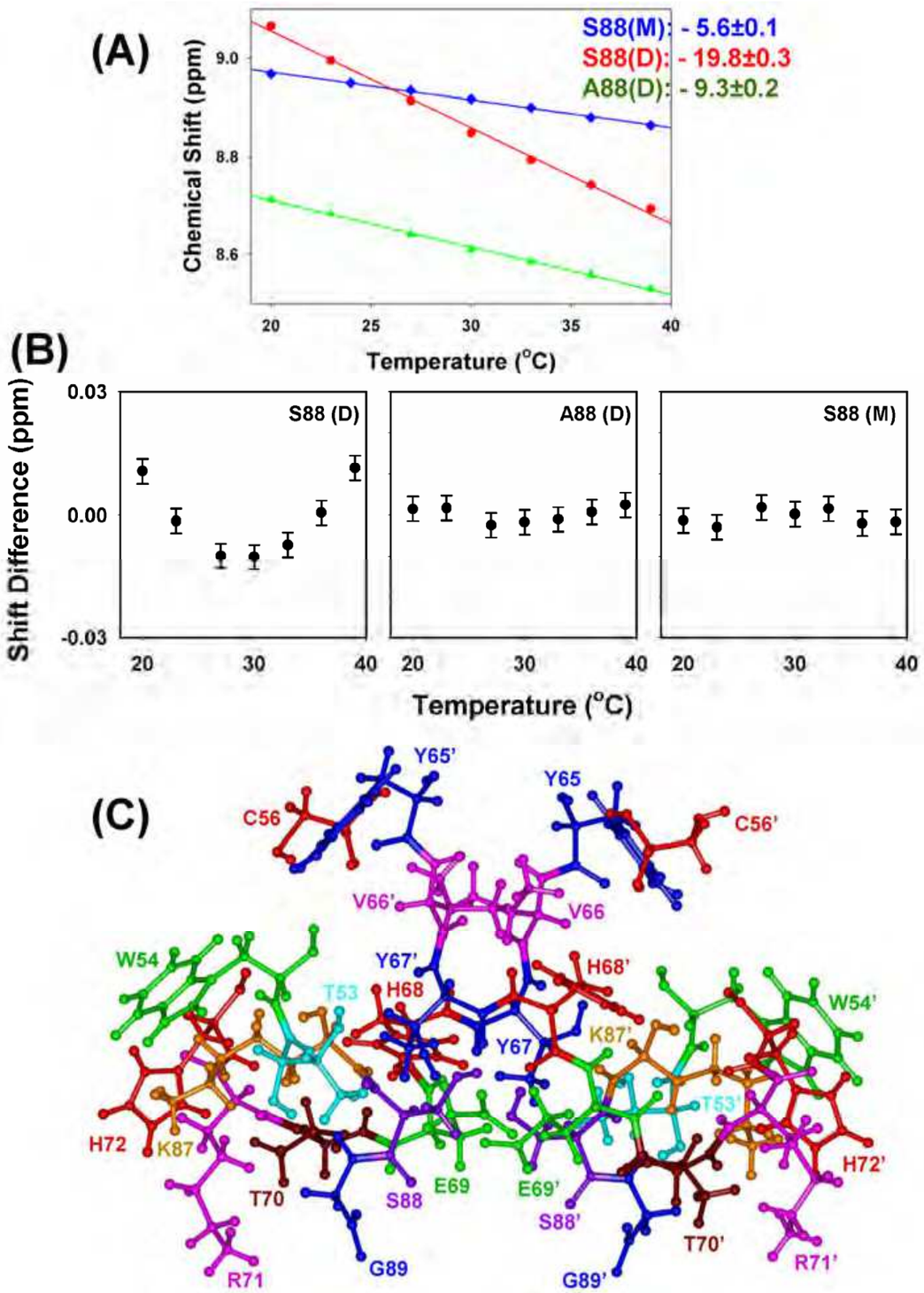

Fig. 8. **(A)** Graph depicting the temperature dependence of amide proton chemical shifts for Ser 88 in DLC8 WT-dimer (Circles, Red), Ala 88 in S88A mutant at pH 7 (Triangles, Green), and Ser 88 in DLC8 monomer at pH 3 (Diamonds, Blue). The solid lines line represents the best linear fit. **(B)** Comparison of non linear/linear temperature dependence of amide

proton chemical shifts at amino acid position 88 in DLC8 protein: Ser 88 in DLC8 WT-dimer [S88-(D)], Ala 88 in S88A mutant [A88-(D)] at pH 7 and Ser 88 in DLC8 monomer [S88-(M)] at pH 3. The measured chemical shifts were fitted to a linear equation. The residuals (observed value – calculated value according to the linear fit) have been plotted against temperature; total scale of y-axis is 0.06 ppm: +0.03 to -0.03 centered at zero, and the temperature range is 18 ^{o}C – 40 ^{o}C. **(C)** Zooming in on a particular region of the dimer interface around Ser 88 in the crystal structure (PDB Id: 1cmi), to show accessibility of the phosphorylation site (side chain –OH of Ser 88) and the interactions of side chains various other residues with Ser 88. Side chains of the residues which are perturbed due to S88A are only shown. The different residues are color coded to indicate the proximity of the side chain atoms of the residue to backbone NH of ser 88; Blue: at least one atom of the side chain is within 2-4 Å, Green: at least one atom of the side chain is within the range 4-6 Å, Red: all atoms are beyond 6 Å.

3.4 Alternative conformations in small globular proteins: Sources of fluctuations and implications to function/folding

Experiments have been performed by various research groups to detect the alternative conformations on different monomeric proteins in order to throw light either on the functional implications or on the folding trajectories. Investigations by Kumar et al (Kumar *et al* 2007) on SUMO-1 suggested that the alternative conformations span the length of the protein chain but are located at particular regions on the protein structure. The authors observed that several of the regions of the protein structure that exhibit such fluctuations coincide with the protein's binding surfaces with different substrate like GTPase effector domain (GED) of dynamin, SUMO binding motifs (SBM), E1 (activating enzyme, SAE1/SAE2) and E2 (conjugating enzyme, UBC9) enzymes of sumoylation machinery and speculated that these conformational fluctuations have significant implications for the binding of diversity of targets by SUMO-1. Another report by Srivastava et al (Srivastava and Chary 2011) on hahellin (a βγ-crystallin domain) in its Ca^{2+}-bound form depicted a large conformational heterogeneity with nearly 40% of the residues, some of which are part of Ca2+-binding loops. Further, they observed that out of the two Greek key motifs, the second Greek key motif is floppy as compared to its counterpart.

Extensive research investigations on theoretical and experimental aspects of different protein systems regarding low-energy excited states have been performed by Williamson and co-workers (Baxter *et al* 1998; Tunnicliffe *et al* 2005; Williamson 2003). Studies on conformational ensemble of cytochrome *c* revealed high structural entropy (Williamson 2003). The density of alternative states is particularly high near the heme ligand Met80, which is of interest because both redox change and the first identified stage in unfolding are associated with change in Met80 ligation. By combining theoretical and experimental approaches, it is concluded that the alternative states each comprise approximately five residues, have in general less structure than the native state and are therefore locally unfolded structures. The locations of the alternative states the global unfolding pathway of cytochrome *c*, hinted that they may determine the pathway. Similar experiments on B1 domains of streptococcal proteins G and L (Tunnicliffe *et al* 2005), which are structurally similar, but have different sequences and folding established that several of the residues

have curved amide proton temperature and indicated approximately 4–6 local minima for each protein. Further, reports on N-terminal domain of phosphoglycerate kinase, hen egg-white lysozyme, SUMO1 and BPTI (Baxter *et al* 1998; Kumar *et al* 2007) established that conformational heterogeneity arises from a number of independent sources such as, aromatic ring current effects, a minor conformer generated through disulphide bond isomerisation; an alternative hydrogen bond network associated with buried water molecules; alternative hydrogen bonds involving backbone amides and surface-exposed side-chain hydrogen bond acceptors; and the disruption of loops, ends of secondary structural elements and chain termini.

In conclusion, on one hand the ruggedness of the native energy landscape of the protein systems provide rationales for the adaptability of the protein structure to bind various target molecules in order to carry out the biological functions efficient manner. On the other hand, it throws light on many potential unfolding initiation sites in the protein. Furthermore, the origins of these conformational fluctuations provide mechanistic insights into the protein network of hydrophobic/H-bond interactions that dictate the protein stability.

4. Abbreviations

NMR - Nuclear magnetic resonance spectroscopy; HSQC - Hetero nuclear single quantum correlation spectroscopy; DLC8 - Dynein light chain protein; *Eh*CaBP - *Entamoeba histolytica* calcium binding protein; Gdmcl - Guanidine Hydrochloride; NCS - Neuronal calcium sensor protein; Myr - Myristoylated; Non-myr - Non-Myristoylated; Pak-1 - P21 activated kinease; SUMO - Small Ubiquitin-like Modifier; BPTI - Bovine pancreatic trypsin inhibitor; UBC9 - Ubiquitin carrier protein 9 .

5. Acknowledgements

The author thank Prof. Ramakrishna V Hosur (TIFR, Mumbai), Prof. K. V. R. Chary (TIFR, Mumbai) for their invaluable guidance, Dr. Sulakshana Mukherjee (UCSD, California) for critical suggestions, the NMR facility at Tata Institute of Fundamental Research (Mumbai, India) and the library facilities at Rutgers University (Piscataway, New Jersey) are greatly acknowledged.

6. References

Ababou A and Desjarlais J R 2001 Solvation energetics and conformational change in EF-hand proteins; *Protein Sci.* 10 301-312.

Agarwal P K 2005 Role of protein dynamics in reaction rate enhancement by enzymes; *J. Am. Chem. Soc.* 127 15248-15256.

Akasaka K 2006 Probing conformational fluctuation of proteins by pressure perturbation; *Chem Rev.* 106 1814-1835.

Alonso C, Miskin J, Hernaez B, Fernandez-Zapatero P, Soto L, Canto C, Rodriguez-Crespo I, Dixon L and Escribano J M 2001 African swine fever virus protein p54 interacts

with the microtubular motor complex through direct binding to light-chain dynein; *J. Virol.* 75 9819-9827.

Andersen N H, Chen C P, Marschner T M, Krystek S R, Jr. and Bassolino D A 1992 Conformational isomerism of endothelin in acidic aqueous media: a quantitative NOESY analysis; *Biochemistry* 31 1280-1295.

Anderson N H, Neidigh J W, Harris S M, Lee G M, Liu Z and Tong H 1997 Extracting information from the temperature gradients of polypeptide HN chemical shifts. 1. The importance of conformational averaging; *J. Am. Chem. Soc.* 119 8547-8561.

Atreya H S, Sahu S C, Bhattacharya A, Chary K V and Govil G 2001 NMR derived solution structure of an EF-hand calcium-binding protein from Entamoeba Histolytica; *Biochemistry* 40 14392-14403.

Bai Y, Sosnick T R, Mayne L and Englander S W 1995 Protein folding intermediates: native-state hydrogen exchange; *Science* 269 192-197.

Barbar E 2008 Dynein light chain LC8 is a dimerization hub essential in diverse protein networks; *Biochemistry* 47 503-508.

Barbar E and Hare M 2004 Characterization of the cargo attachment complex of cytoplasmic dynein using NMR and mass spectrometry; *Methods Enzymol.* 380 219-241.

Baxter N J, Hosszu L L, Waltho J P and Williamson M P 1998 Characterisation of low free-energy excited states of folded proteins; *J. Mol. Biol.* 284 1625-1639.

Baxter N J and Williamson M P 1997 Temperature dependence of 1H chemical shifts in proteins; *J. Biomol. NMR* 9 359-369.

Bhabha G, Lee J, Ekiert D C, Gam J, Wilson I A, Dyson H J, Benkovic S J and Wright P E 2011 A dynamic knockout reveals that conformational fluctuations influence the chemical step of enzyme catalysis; *Science* 332 234-238.

Bhattacharya A, Padhan N, Jain R and Bhattacharya S 2006 Calcium-binding proteins of Entamoeba histolytica; *Arch. Med. Res.* 37 221-225.

Bhattacharya S, Bunick C G and Chazin W J 2004 Target selectivity in EF-hand calcium binding proteins; *Biochim. Biophys. Acta* 1742 69-79.

Boehr D D, McElheny D, Dyson H J and Wright P E 2006 The dynamic energy landscape of dihydrofolate reductase catalysis; *Science* 313 1638-1642.

Boehr D D, McElheny D, Dyson H J and Wright P E 2010 Millisecond timescale fluctuations in dihydrofolate reductase are exquisitely sensitive to the bound ligands; *Proc. Natl. Acad. Sci. U. S. A* 107 1373-1378.

Bryngelson J D, Onuchic J N, Socci N D and Wolynes P G 1995 Funnels, pathways, and the energy landscape of protein folding: a synthesis; *Proteins* 21 167-195.

Buck T M, Wagner J, Grund S and Skach W R 2007 A novel tripartite motif involved in aquaporin topogenesis, monomer folding and tetramerization; *Nat. Struct. Mol. Biol.* 14 762-769.

Chandra K, Sharma Y and Chary K V 2011 Characterization of low-energy excited states in the native state ensemble of non-myristoylated and myristoylated neuronal calcium sensor-1; *Biochim. Biophys. Acta* 1814 334-344.

Chatterjee A, Krishna Mohan P M, Prabhu A, Ghosh-Roy A and Hosur R V 2007 Equilibrium unfolding of DLC8 monomer by urea and guanidine hydrochloride: Distinctive global and residue level features; *Biochimie* 89 117-134.

Cierpicki T and Otlewski J 2001 Amide proton temperature coefficients as hydrogen bond indicators in proteins; *J. Biomol. NMR* 21 249-261.

Cierpicki T, Zhukov I, Byrd R A and Otlewski J 2002 Hydrogen bonds in human ubiquitin reflected in temperature coefficients of amide protons; *J. Magn Reson.* 157 178-180.

Clore G M 2011 Exploring sparsely populated states of macromolecules by diamagnetic and paramagnetic NMR relaxation; *Protein Sci.* 20 229-246.

Clore G M and Iwahara J 2009 Theory, practice, and applications of paramagnetic relaxation enhancement for the characterization of transient low-population states of biological macromolecules and their complexes; *Chem. Rev.* 109 4108-4139.

Dill K A and Chan H S 1997 From Levinthal to pathways to funnels; *Nat. Struct. Biol.* 4 10-19.

Dobson C M 2003 Protein folding and misfolding; *Nature* 426 884-890.

Dobson C M and Karplus M 1999 The fundamentals of protein folding: bringing together theory and experiment; *Curr. Opin. Struct. Biol.* 9 92-101.

Dunker A K, Brown C J, Lawson J D, Iakoucheva L M and Obradovic Z 2002 Intrinsic disorder and protein function; *Biochemistry* 41 6573-6582.

Dyson H J and Wright P E 2005 Elucidation of the protein folding landscape by NMR; *Methods Enzymol.* 394 299-321.

Eisenmesser E Z, Millet O, Labeikovsky W, Korzhnev D M, Wolf-Watz M, Bosco D A, Skalicky J J, Kay L E and Kern D 2005 Intrinsic dynamics of an enzyme underlies catalysis; *Nature* 438 117-121.

Fan J, Zhang Q, Tochio H, Li M and Zhang M 2001 Structural basis of diverse sequence-dependent target recognition by the 8 kDa dynein light chain; *J. Mol. Biol.* 306 97-108.

Fan J S, Zhang Q, Li M, Tochio H, Yamazaki T, Shimizu M and Zhang M 1998 Protein inhibitor of neuronal nitric-oxide synthase, PIN, binds to a 17-amino acid residue fragment of the enzyme; *J. Biol. Chem.* 273 33472-33481.

Feher V A and Cavanagh J 1999 Millisecond-timescale motions contribute to the function of the bacterial response regulator protein Spo0F; *Nature* 400 289-293.

Finn B E, Evenas J, Drakenberg T, Waltho J P, Thulin E and Forsen S 1995 Calcium-induced structural changes and domain autonomy in calmodulin; *Nat. Struct. Biol.* 2 777-783.

Frankel B A, Tong Y, Bentley M L, Fitzgerald M C and McCafferty D G 2007 Mutational analysis of active site residues in the Staphylococcus aureus transpeptidase SrtA; *Biochemistry* 46 7269-7278.

Fraser J S, Clarkson M W, Degnan S C, Erion R, Kern D and Alber T 2009 Hidden alternative structures of proline isomerase essential for catalysis; *Nature* 462 669-673.

Fuhrmann J C, Kins S, Rostaing P, El F O, Kirsch J, Sheng M, Triller A, Betz H and Kneussel M 2002 Gephyrin interacts with Dynein light chains 1 and 2, components of motor protein complexes; *J. Neurosci.* 22 5393-5402.

Grant M A, Lazo N D, Lomakin A, Condron M M, Arai H, Yamin G, Rigby A C and Teplow D B 2007 Familial Alzheimer's disease mutations alter the stability of the amyloid beta-protein monomer folding nucleus; *Proc. Natl. Acad. Sci. U. S. A* 104 16522-16527.

Hackney C M, Mahendrasingam S, Penn A and Fettiplace R 2005 The concentrations of calcium buffering proteins in mammalian cochlear hair cells; *J. Neurosci.* 25 7867-7875.

Hanley J G and Henley J M 2005 PICK1 is a calcium-sensor for NMDA-induced AMPA receptor trafficking; *EMBO J.* 24 3266-3278.

Heizmann C W 1992 Calcium-binding proteins: basic concepts and clinical implications; *Gen. Physiol Biophys.* 11 411-425.

Heizmann C W and Schafer B W 1990 Internal calcium-binding proteins; *Semin. Cell Biol.* 1 277-282.

Hilge M, Aelen J and Vuister G W 2006 Ca2+ regulation in the Na+/Ca2+ exchanger involves two markedly different Ca2+ sensors; *Mol. Cell* 22 15-25.

Ishibashi M, Tatsuda S, Izutsu K, Kumeda K, Arakawa T and Tokunaga M 2007 A single Gly114Arg mutation stabilizes the hexameric subunit assembly and changes the substrate specificity of halo-archaeal nucleoside diphosphate kinase; *FEBS Lett.* 581 4073-4079.

Jaffrey S R and Snyder S H 1996 PIN: an associated protein inhibitor of neuronal nitric oxide synthase; *Science* 274 774-777.

Kitahara R, Yokoyama S and Akasaka K 2005 NMR snapshots of a fluctuating protein structure: ubiquitin at 30 bar-3 kbar; *J. Mol. Biol.* 347 277-285.

Korzhnev D M, Karlsson B G, Orekhov V Y and Billeter M 2003 NMR detection of multiple transitions to low-populated states in azurin; *Protein Sci.* 12 56-65.

Kretsinger R H and Nockolds C E 1973 Carp muscle calcium-binding protein. II. Structure determination and general description; *J. Biol. Chem.* 248 3313-3326.

Krishna Mohan P M, Barve M, Chatterjee A, Ghosh-Roy A and Hosur R V 2008 NMR comparison of the native energy landscapes of DLC8 dimer and monomer; *Biophys. Chem* 134 10-19.

Kumar A, Srivastava S and Hosur R V 2007 NMR characterization of the energy landscape of SUMO-1 in the native-state ensemble; *J. Mol. Biol.* 367 1480-1493.

Lambers T T, Mahieu F, Oancea E, Hoofd L, de L F, Mensenkamp A R, Voets T, Nilius B, Clapham D E, Hoenderop J G and Bindels R J 2006 Calbindin-D28K dynamically controls TRPV5-mediated Ca2+ transport; *EMBO J.* 25 2978-2988.

Levinthal C 1969. Mössbauer Spectroscopy in Biological Systems. (eds. DeBrunner JTP and Munck E), pp 22-24. University of Illinois Press: Illinois.

Liang J, Jaffrey S R, Guo W, Snyder S H and Clardy J 1999 Structure of the PIN/LC8 dimer with a bound peptide; *Nat. Struct. Biol.* 6 735-740.

Lo K W, Naisbitt S, Fan J S, Sheng M and Zhang M 2001 The 8-kDa dynein light chain binds to its targets via a conserved (K/R)XTQT motif; *J. Biol. Chem.* 276 14059-14066.

Makokha M, Huang Y J, Montelione G, Edison A S and Barbar E 2004 The solution structure of the pH-induced monomer of dynein light-chain LC8 from Drosophila; *Protein Sci.* 13 727-734.

Mittermaier A and Kay L E 2006 New tools provide new insights in NMR studies of protein dynamics; *Science* 312 224-228.

Mohan P M, Barve M, Chatterjee A and Hosur R V 2006 pH driven conformational dynamics and dimer-to-monomer transition in DLC8; *Protein Sci.* 15 335-342.

Mohan P M, Chakraborty S and Hosur R V 2008a Residue-wise conformational stability of DLC8 dimer from native-state hydrogen exchange; *Proteins*.

Mohan P M and Hosur R V 2008 NMR characterization of structural and dynamics perturbations due to a single point mutation in Drosophila DLC8 dimer: functional implications; *Biochemistry* 47 6251-6259.

Mohan P M, Mukherjee S and Chary K V 2008b Differential native state ruggedness of the two Ca2+-binding domains in a Ca2+ sensor protein; *Proteins* 70 1147-1153.

Mukherjee S, Kuchroo K and Chary K V 2005 Structural characterization of the apo form of a calcium binding protein from Entamoeba histolytica by hydrogen exchange and its folding to the holo state; *Biochemistry* 44 11636-11645.

Mukherjee S, Mohan P M and Chary K V 2007a Magnesium promotes structural integrity and conformational switching action of a calcium sensor protein; *Biochemistry* 46 3835-3845.

Mukherjee S, Mohan P M, Kuchroo K and Chary K V 2007b Energetics of the native energy landscape of a two-domain calcium sensor protein: distinct folding features of the two domains; *Biochemistry* 46 9911-9919.

Naisbitt S, Valtschanoff J, Allison D W, Sala C, Kim E, Craig A M, Weinberg R J and Sheng M 2000 Interaction of the postsynaptic density-95/guanylate kinase domain-associated protein complex with a light chain of myosin-V and dynein; *J. Neurosci.* 20 4524-4534.

Nelson M R and Chazin W J 1998 Structures of EF-hand Ca(2+)-binding proteins: diversity in the organization, packing and response to Ca2+ binding; *Biometals* 11 297-318.

Nyarko A, Cochrun L, Norwood S, Pursifull N, Voth A and Barbar E 2005 Ionization of His 55 at the dimer interface of dynein light-chain LC8 is coupled to dimer dissociation; *Biochemistry* 44 14248-14255.

Onuchic J N, Luthey-Schulten Z and Wolynes P G 1997 Theory of protein folding: the energy landscape perspective; *Annu. Rev. Phys. Chem.* 48 545-600.

Parak F G 2003a Proteins in action: the physics of structural fluctuations and conformational changes; *Curr. Opin. Struct. Biol.* 13 552-557.

Parak F G 2003b Proteins in action: the physics of structural fluctuations and conformational changes; *Curr. Opin. Struct. Biol.* 13 552-557.

Piana S, Carloni P and Parrinello M 2002 Role of conformational fluctuations in the enzymatic reaction of HIV-1 protease; *J. Mol. Biol.* 319 567-583.

Piana S, Laio A, Marinelli F, Van T M, Bourry D, Ampe C and Martins J C 2008 Predicting the effect of a point mutation on a protein fold: the villin and advillin headpieces and their Pro62Ala mutants; *J. Mol. Biol.* 375 460-470.

Popovych N, Sun S, Ebright R H and Kalodimos C G 2006 Dynamically driven protein allostery; *Nat. Struct. Mol. Biol.* 13 831-838.

Puthalakath H, Huang D C, O'Reilly L A, King S M and Strasser A 1999 The proapoptotic activity of the Bcl-2 family member Bim is regulated by interaction with the dynein motor complex; *Mol. Cell* 3 287-296.

Riley P W, Cheng H, Samuel D, Roder H and Walsh P N 2007 Dimer dissociation and unfolding mechanism of coagulation factor XI apple 4 domain: spectroscopic and mutational analysis; *J. Mol. Biol.* 367 558-573.

Rosenbaum E E, Hardie R C and Colley N J 2006 Calnexin is essential for rhodopsin maturation, Ca2+ regulation, and photoreceptor cell survival; *Neuron* 49 229-241.

Schwarzinger S, Kroon G J, Foss T R, Chung J, Wright P E and Dyson H J 2001 Sequence-dependent correction of random coil NMR chemical shifts; *J. Am. Chem. Soc.* 123 2970-2978.

Schwarzinger S, Kroon G J, Foss T R, Wright P E and Dyson H J 2000 Random coil chemical shifts in acidic 8 M urea: implementation of random coil shift data in NMRView; *J. Biomol. NMR* 18 43-48.

Shaw G S, Hodges R S and Sykes B D 1990 Calcium-induced peptide association to form an intact protein domain: 1H NMR structural evidence; *Science* 249 280-283.

Shoemaker B A, Wang J and Wolynes P G 1999 Exploring structures in protein folding funnels with free energy functionals: the transition state ensemble; *J. Mol. Biol.* 287 675-694.

Song C, Wen W, Rayala S K, Chen M, Ma J, Zhang M and Kumar R 2008 Serine 88 Phosphorylation of the 8-kDa Dynein Light Chain 1 Is a Molecular Switch for Its Dimerization Status and Functions; *J. Biol. Chem* 283 4004-4013.

Song Y, Benison G, Nyarko A, Hays T S and Barbar E 2007 Potential role for phosphorylation in differential regulation of the assembly of dynein light chains; *J. Biol. Chem* 282 17272-17279.

Spitzer J J and Poolman B 2005 Electrochemical structure of the crowded cytoplasm; *Trends Biochem. Sci.* 30 536-541.

Srivastava A K and Chary K V 2011 Conformational heterogeneity and dynamics in a betagamma-Crystallin from Hahella chejuensis; *Biophys. Chem.* 157 7-15.

Stewart A K, Boyd C A and Vaughan-Jones R D 1999 A novel role for carbonic anhydrase: cytoplasmic pH gradient dissipation in mouse small intestinal enterocytes; *J. Physiol* 516 (Pt 1) 209-217.

Stollar E J, Mayor U, Lovell S C, Federici L, Freund S M, Fersht A R and Luisi B F 2003 Crystal structures of engrailed homeodomain mutants: implications for stability and dynamics; *J. Biol. Chem* 278 43699-43708.

Strynadka N C and James M N 1989 Crystal structures of the helix-loop-helix calcium-binding proteins; *Annu. Rev. Biochem.* 58 951-998.

Swietach P, Leem C H, Spitzer K W and Vaughan-Jones R D 2005 Experimental generation and computational modeling of intracellular pH gradients in cardiac myocytes; *Biophys. J.* 88 3018-3037.

Swietach P and Vaughan-Jones R D 2004 Novel method for measuring junctional proton permeation in isolated ventricular myocyte cell pairs; *Am. J. Physiol Heart Circ. Physiol* 287 H2352-H2363.

Tang C, Louis J M, Aniana A, Suh J Y and Clore G M 2008 Visualizing transient events in amino-terminal autoprocessing of HIV-1 protease; *Nature* 455 693-696.

Tilton R F, Jr., Dewan J C and Petsko G A 1992 Effects of temperature on protein structure and dynamics: X-ray crystallographic studies of the protein ribonuclease-A at nine different temperatures from 98 to 320 K; *Biochemistry* 31 2469-2481.

Tobi D and Bahar I 2005 Structural changes involved in protein binding correlate with intrinsic motions of proteins in the unbound state; *Proc. Natl. Acad. Sci. U. S. A* 102 18908-18913.

Tunnicliffe R B, Waby J L, Williams R J and Williamson M P 2005 An experimental investigation of conformational fluctuations in proteins G and L; *Structure. (Camb.)* 13 1677-1684.

Tzeng S R and Kalodimos C G 2009 Dynamic activation of an allosteric regulatory protein; *Nature* 462 368-372.

Uversky V N 2002 Natively unfolded proteins: a point where biology waits for physics; *Protein Sci.* 11 739-756.

Uversky V N 2003 Protein folding revisited. A polypeptide chain at the folding-misfolding-nonfolding cross-roads: which way to go?; *Cell Mol. Life Sci.* 60 1852-1871.

Vadlamudi R K, Bagheri-Yarmand R, Yang Z, Balasenthil S, Nguyen D, Sahin A A, den H P and Kumar R 2004 Dynein light chain 1, a p21-activated kinase 1-interacting substrate, promotes cancerous phenotypes; *Cancer Cell* 5 575-585.

Vaughan-Jones R D, Peercy B E, Keener J P and Spitzer K W 2002 Intrinsic H(+) ion mobility in the rabbit ventricular myocyte; *J. Physiol* 541 139-158.

Villali J and Kern D 2010 Choreographing an enzyme's dance; *Curr. Opin. Chem. Biol.* 14 636-643.

Vinogradova M V, Stone D B, Malanina G G, Karatzaferi C, Cooke R, Mendelson R A and Fletterick R J 2005 Ca(2+)-regulated structural changes in troponin; *Proc. Natl. Acad. Sci. U. S. A* 102 5038-5043.

Whitten S T, Garcia-Moreno E B and Hilser V J 2005 Local conformational fluctuations can modulate the coupling between proton binding and global structural transitions in proteins; *Proc. Natl. Acad. Sci. U. S. A* 102 4282-4287.

Williamson M P 2003 Many residues in cytochrome c populate alternative states under equilibrium conditions; *Proteins* 53 731-739.

Williamson M P, Hall M J and Handa B K 1986 1H-NMR assignment and secondary structure of a herpes simplex virus glycoprotein D-1 antigenic domain; *Eur. J. Biochem.* 158 527-536.

Willoughby D and Schwiening C J 2002 Electrically evoked dendritic pH transients in rat cerebellar Purkinje cells; *J. Physiol* 544 487-499.

Wishart D S, Bigam C G, Holm A, Hodges R S and Sykes B D 1995 1H, 13C and 15N random coil NMR chemical shifts of the common amino acids. I. Investigations of nearest-neighbor effects; *J. Biomol. NMR* 5 67-81.

Wishart D S and Sykes B D 1994 Chemical shifts as a tool for structure determination; *Methods Enzymol.* 239 363-392.

Wolynes P G 2005 Energy landscapes and solved protein-folding problems; *Philos. Transact. A Math. Phys. Eng Sci.* 363 453-464.

Wolynes P G, Onuchic J N and Thirumalai D 1995 Navigating the folding routes; *Science* 267 1619-1620.

Wüthrich K 1986. *NMR of protein and nucleic acids*. John Wiley and Sons: New York.

Yang Z, Vadlamudi R K and Kumar R 2005 Dynein light chain 1 phosphorylation controls macropinocytosis; *J. Biol. Chem* 280 654-659.

Zaniboni M, Swietach P, Rossini A, Yamamoto T, Spitzer K W and Vaughan-Jones R D 2003 Intracellular proton mobility and buffering power in cardiac ventricular myocytes from rat, rabbit, and guinea pig; *Am. J. Physiol Heart Circ. Physiol* 285 H1236-H1246.

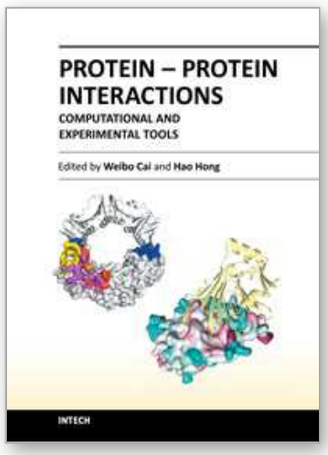

Protein-Protein Interactions - Computational and Experimental Tools

Edited by Dr. Weibo Cai

ISBN 978-953-51-0397-4
Hard cover, 472 pages
Publisher InTech
Published online 30, March, 2012
Published in print edition March, 2012

Proteins are indispensable players in virtually all biological events. The functions of proteins are coordinated through intricate regulatory networks of transient protein-protein interactions (PPIs). To predict and/or study PPIs, a wide variety of techniques have been developed over the last several decades. Many in vitro and in vivo assays have been implemented to explore the mechanism of these ubiquitous interactions. However, despite significant advances in these experimental approaches, many limitations exist such as false-positives/false-negatives, difficulty in obtaining crystal structures of proteins, challenges in the detection of transient PPI, among others. To overcome these limitations, many computational approaches have been developed which are becoming increasingly widely used to facilitate the investigation of PPIs. This book has gathered an ensemble of experts in the field, in 22 chapters, which have been broadly categorized into Computational Approaches, Experimental Approaches, and Others.

How to reference

In order to correctly reference this scholarly work, feel free to copy and paste the following:

Maruthi Krishna Mohan Poluri (2012). NMR Investigations on Ruggedness of Native State Energy Landscape in Folded Proteins, Protein-Protein Interactions - Computational and Experimental Tools, Dr. Weibo Cai (Ed.), ISBN: 978-953-51-0397-4, InTech, Available from: http://www.intechopen.com/books/protein-protein-interactions-computational-and-experimental-tools/nmr-investigations-on-ruggedness-of-native-state-energy-landscape-in-folded-proteins

INTECH
open science | open minds

InTech Europe
University Campus STeP Ri
Slavka Krautzeka 83/A
51000 Rijeka, Croatia
Phone: +385 (51) 770 447
Fax: +385 (51) 686 166
www.intechopen.com

InTech China
Unit 405, Office Block, Hotel Equatorial Shanghai
No.65, Yan An Road (West), Shanghai, 200040, China
中国上海市延安西路65号上海国际贵都大饭店办公楼405单元
Phone: +86-21-62489820
Fax: +86-21-62489821

IntechOpen